PCCP

PAPER

View Article Online
View Journal | View Issue

Cite this: *Phys. Chem. Chem. Phys.*, 2017, **19**, 19937

Adsorption of galloyl catechin aggregates significantly modulates membrane mechanics in the absence of biochemical cues†

Takahisa Matsuzaki,[ab] Hiroaki Ito,[bc] Veronika Chevyreva,[b] Ali Makky,[bd] Stefan Kaufmann,[b] Kazuki Okano,[a] Naritaka Kobayashi,[e] Masami Suganuma,[e] Seiichiro Nakabayashi,[a] Hiroshi Y. Yoshikawa *[a] and Motomu Tanaka *[bf]

Received 28th April 2017,
Accepted 7th July 2017

DOI: 10.1039/c7cp02771k

rsc.li/pccp

Physical interactions of four major green tea catechin derivatives with cell membrane models were systemically investigated. Catechins with the galloyl moiety caused the aggregation of small unilamellar vesicles and an increase in the surface pressure of lipid monolayers, while those without did not. Differential scanning calorimetry revealed that, in a low concentration regime ($\leq$10 μM), catechin molecules are not significantly incorporated into the hydrophobic core of lipid membranes as substitutional impurities. Partition coefficient measurements revealed that the galloyl moiety of catechin and the cationic quaternary amine of lipids dominate the catechin–membrane interaction, which can be attributed to the combination of electrostatic and cation–π interactions. Finally, we shed light on the mechanical consequence of catechin–membrane interactions using the Fourier-transformation of the membrane fluctuation. Surprisingly, the incubation of cell-sized vesicles with 1 μM galloyl catechins, which is comparable to the level in human blood plasma after green tea consumption, significantly increased the bending stiffness of the membranes by a factor of more than 60, while those without the galloyl moiety had no detectable influence. Atomic force microscopy and circular dichroism spectroscopy suggest that the membrane stiffening is mainly attributed to the adsorption of galloyl catechin aggregates to the membrane surfaces. These results contribute to our understanding of the physical and thus the generic functions of green tea catechins in therapeutics, such as cancer prevention.

1. Introduction

(−)-Epigallocatechin gallate (EGCG) is the most abundant catechin in green tea extract and known to exhibit a wide range of pharmaceutical functions such as antibacterial effects[1–3] and cancer prevention.[4–6] To date, many studies have tried to elucidate the functions of EGCG biochemically, *e.g.* antioxidant activity[7–9] and specific inhibition of tumor-related proteins.[10–12] On the other hand, there have been only few groups that shed light on the physical mechanism of interactions between EGCG and cell membranes.

Tamba *et al.* reported that the mixing of EGCG and giant vesicles caused the aggregation and lysis of membranes.[13] Sun *et al.* utilized X-ray diffraction and micropipette aspiration, and reported that EGCG leads to the thinning of egg-phosphatidylcholine (egg-PC) bilayers without significant areal expansion, suggesting the partial solubilization of lipids.[14] NMR studies suggested that the galloyl moiety might interact with phospholipids *via* either hydrophobic interaction and/or cation–π interaction.[15] This seems consistent with the fact that catechin derivatives with the galloyl moiety, such as EGCG and (−)-epicatechin gallate (ECG), show higher pharmaceutical efficacies compared to those without the galloyl moiety.[16–20] The Nakayama group tried to compare the affinity of different types of catechin derivatives for small unilamellar vesicles (SUVs) of egg-PC using a high performance liquid chromatography (HPLC) assay,[21] and tried to evaluate the interactions of catechins with DMPC (1,2-dimyristoyl-*sn-glycero*-3-phosphocholine) multibilayers by quartz crystal microbalance (QCM).[22] But, the former

[a] *Department of Chemistry, Saitama University, Sakura-ku, Saitama, 338-8570, Japan. E-mail: hiroshi@mail.saitama-u.ac.jp; Tel: +81-(0)-48-858-3379*
[b] *Physical Chemistry of Biosystems, Institute of Physical Chemistry, Heidelberg University, D69120 Heidelberg, Germany. E-mail: tanaka@uni-heidelberg.de; Fax: +49-(0)-6221-544918; Tel: +49-(0)-6221-544916*
[c] *Department of Physics, Graduate School of Science, Kyoto University, Kyoto 606-8502, Japan*
[d] *Institut Galien Paris-Sud, CNRS, Univ. Paris-Sud, University Paris-Saclay, 92296 Châtenay-Malabry, France*
[e] *Graduate School of Science and Engineering, Saitama University, Shimo-okubo 255, Sakura-ku, Saitama 338-8570, Japan*
[f] *Institute for Integrated Cell-Material Sciences (WPI iCeMS), Kyoto University, 606-8501, Kyoto, Japan*

† Electronic supplementary information (ESI) available. See DOI: 10.1039/c7cp02771k

suffered from the lack of quantitative values due to ill-defined lipid mixtures in egg-PC, and the latter from uncertainty in estimating the area of lipid multilayers. From this context, the quantitative assessment of differential interactions of catechin derivatives with cell membranes is still missing.

Another open question is, how much do the physical interactions of catechin derivatives influence the mechanical properties of lipid membranes? Recent studies showed considerable evidence that some catechin derivatives can stiffen metastatic cancer cells and reduce their motility.[23] Gimzewski *et al.* explained that such stiffening of cancer cells in terms of the elevated expression of cytoskeletal F-actin.[24] However, considering the structures of catechin derivatives, it is also plausible that catechin derivatives directly influence the membrane mechanics *via* adsorption onto and/or incorporation into lipid membranes. Although catechin derivatives with a galloyl moiety were found to alter the fluidity and molecular packing of membranes by using fluorescence spectroscopy techniques,[25–27] there have been no quantitative studies on the influence of catechin derivatives on the membrane mechanics.

In this work, we systematically studied how four major catechin derivatives in green tea, EGCG, ECG, (−)-epigallocatechin (EGC), and (−)-epicatechin (EC), physically interact with cell membrane models (Fig. 1). The reaction kinetics of catechin–membrane interaction was monitored by measuring dynamic light scattering (DLS) over time. To assess the influence of the catechin derivatives on membrane surface tension and molecular cooperativity, the surface pressure and thermotropic phase behavior of the lipid membranes in the absence and presence of the catechin derivatives were measured by film balance experiments and differential scanning calorimetry (DSC), respectively. In addition, the affinity of the catechin derivatives to the lipid membranes was evaluated as partition coefficients by using particle-supported membranes.

Finally, the impact of the catechin derivatives on the mechanical properties of lipid membranes has been studied by flicker spectroscopy for the first time.[28–32] This method allows us to determine the bending stiffness of giant unilamellar vesicle (GUV) membranes at physiological temperature (37 °C) by Fourier analysis of thermally excited membrane fluctuation.

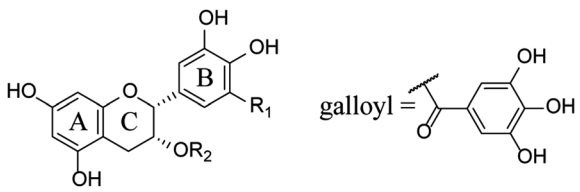

Name	R_1	R_2
(−)-Epigallocatechin gallate (EGCG)	OH	galloyl
(−)-Epicatechin gallate (ECG)	H	galloyl
(−)-Epigallocatechin (EGC)	OH	H
(−)-Epicatechin (EC)	H	H

Fig. 1 Molecular structures of the four major catechin derivatives used in this study.

In contrast to alternative approaches by applying external forces with an atomic force microscope,[33] electric fields,[34] magnetic tweezers,[35] and optical stretchers,[36] flicker spectroscopy is a label/probe-free technique that ensures the quantitative determination of membrane mechanics without disturbing the physical interaction between lipid membranes and catechin derivatives. We also discussed the mechanism of the changes detected in the membrane mechanics with the catechin derivatives from the viewpoint of structures of catechin aggregates, which could be revealed by atomic force microscopy (AFM) and circular dichroism (CD) spectroscopy.

2. Materials and methods

Materials

Deionized water from a Milli-Q device (Millipore, Molsheim, France) was used throughout this study. Unless stated otherwise, all other chemicals were purchased either from Sigma-Aldrich (Munich, Germany), Carl Roth (Karlsruhe, Germany) or Wako Pure Chemicals (Tokyo, Japan) and were used without further purification. Chloroform solutions of lipids were purchased from Avanti Polar Lipids (AL, USA).

Preparation of catechin solutions

Four different catechin derivatives, EGCG (Sigma Aldrich, Munich, Germany), ECG (Wako, Tokyo, Japan), EGC (Wako, Tokyo, Japan), and EC (Sigma Aldrich, Munich, Germany), were used. Catechin powder was thoroughly dissolved in trifluoroethanol (TFE, Sigma Aldrich, Munich, Germany), which can enhance the dispersion of EGCG (Fig. S1, ESI†). Then the catechin solution was mixed with a filtered HEPES buffer (10 mM HEPES, 150 mM KCl, 0.1 mM EDTA, pH 7.4) and immediately used for experiments. Fluorescence and CD spectra were measured using a fluorometer (LP-6300, JASCO Co., Tokyo, Japan) and spectropolarimeter (J-600, JASCO, Tokyo, Japan), respectively.

Preparation of vesicle suspensions

A lipid stock solution in chloroform (2.5 mg mL^{-1}) was placed in a vacuum rotary evaporator and kept in a vacuum oven overnight. The dried lipid films were re-suspended in a 10 mM HEPES buffer for ~15 min. Small unilamellar vesicle (SUV) suspensions were prepared either by (i) extrusion[37,38] or (ii) ultrasonication.[39,40] In brief, (i) lipid suspensions were extruded through a polycarbonate filter with a pore diameter of 100 nm (LiposoFast, Avanti, AL, USA); and (ii) to prepare smaller SUVs with a diameter of ~40 nm, lipid suspensions were sonicated with a tip sonicator (Misonix, New York, USA) for approximately 1.5 h until the solution became transparent.

Giant unilamellar vesicles (GUVs, $\Phi \sim 20$ μm) were prepared by the electro-swelling method.[41,42] After spin-coating lipid chloroform solutions on ITO substrates (300 rpm, 10 min), the lipid films were hydrated with 300 mM sucrose solutions under AC potentials (10 kHz, 1.5 V) for 2 h at 37 °C. The GUV suspension (0.2 mL) was mixed with a 360 mM glucose solution (1 mL) to gain a better image contrast for phase contrast microscopy and to accelerate the sedimentation of GUVs.

Dynamic light scattering (DLS)

Six μL of catechin solutions (6 mM) were mixed with 394 μL of 2 mM OPPC (1-oleoyl-2-palmitoyl-*sn-glycero*-3-phosphocholine) SUV solution. The mixed solutions were incubated for 3 h at 20 °C. Finally, the mixture was measured with a Zetasizer Nano (Malvern, Worcestershire, UK) at 20 °C. The mean diameter $\langle D\rangle$ of the vesicles (normalized by volume) was calculated according to eqn (1):

$$\langle D\rangle = \frac{\sum V_i D_i}{\sum V_i} \quad (1)$$

V_i is the volume fraction of vesicles with a diameter of D_i from the size distribution. The standard deviation, σ, of $\langle D\rangle$ was calculated according to eqn (2):

$$\sigma = \sqrt{\frac{\sum (D_i - \langle D\rangle)^2 V_i}{\sum V_i}} \quad (2)$$

The time evolution of $\langle D\rangle$ was fitted with an exponential function:

$$\langle D(t)\rangle = D(t = \infty) + (a - D(t = \infty)) \times e^{-t/\tau} \quad (3)$$

where τ is characteristic time constant. Plots of $\langle D\rangle$ *vs.* catechin concentration (c) were fitted with a sigmoidal function:

$$\langle D(c)\rangle = a' + \{(D(c = \infty) - a')/(1 + e^{(c_{half} - c)/b'})\} \quad (4)$$

where the half-saturation level c_{half} represents the critical concentration that causes vesicle aggregation.

Film balance experiment

A MicroTrough X film balance (Kibron Inc., Espoo, Finland) was used to monitor the surface pressure of the lipid monolayer at air/water interfaces. Seventeen μL of OPPC chloroform solution (1 mg mL^{-1}) was deposited on 20 mL of 10 mM HEPES buffer at 20 °C and kept for 10 min to evaporate the solvent. The film was then compressed at a constant speed of ~3 Å^2 per chain per min until it reached a surface pressure of ~20 mN m^{-1}. After confirming the film stability, 3–333 μL of catechin solution (6 mM) was injected into the subphase to achieve a final concentration of 1–100 μM. It should be noted that none of the catechin derivatives show surface activity up to a concentration of 100 μM (Fig. S2, ESI†).[43] In addition, we confirmed that TFE does not cause any detectable change in the surface pressures of lipid monolayers (Fig. S3 ESI†).

Differential scanning calorimetry (DSC)

A 492 μL portion of 2 mM SOPC (1-stearoyl-2-oleoyl-*sn-glycero*-3-phosphocholine) SUV solution was mixed with 8 μL of catechin solutions (0.6 mM). The mixed solutions were incubated for 3 h at 20 °C. The mixture (500 μL) was then placed in a VP-DSC MicroCalorimeter (MicroCal, Northampton, USA), and heat capacity scans were recorded. To ensure the thermal equilibrium, at least two successive heating/cooling scans were recorded between 3 and 9 °C at a scan rate of 10 °C h^{-1}. The main phase transition temperature of SOPC was higher enough than the OPPC one to be fully within the detection range of the device.

Partition coefficient measurements of the catechin derivatives in lipid membranes

The association of the catechin derivatives with lipid membranes was evaluated using partition coefficients. Here, we prepared SUV suspensions (4 mM) of zwitterionic DOPC (1,2-dioleoyl-*sn-glycero*-3-phosphocholine) and those containing 30 mol% of either DOPE (1,2-dioleoyl-*sn-glycero*-3-phosphoethanolamine) as zwitterionic (±), DOTAP (1,2-dioleoyl-3-trimethylammonium-propane) as cationic (+), or DOPG (1,2-di-(9Z-octadecenoyl)-*sn-glycero*-3-phospho-(1′-*rac*-glycerol)) as anionic (−) lipids. To deposit lipid bilayers on the surface of silica particles, SUV suspensions were mixed with porous silica beads (Φ = 5 μm, pore size = 30 nm, Kromasil, Akzo Nobel Chemicals, Mannheim, Germany) by using a rotary shaker overnight.[44–46] The concentration of the silica beads after the mixing was 10 mg mL^{-1}. We confirmed that the surface of the silica beads was fully covered with lipids by fluorescence microscopy (Fig. S4, ESI†). The beads were sedimented by centrifugation for 30 s at 10 000 rpm. The sample was washed with a 10 mM HEPES buffer three times. One mL of lipid-coated bead suspension was mixed with 16.6 μL of catechin solutions (0.6 mM) by using a rotary shaker for 3 h at 20 °C. The solution was centrifuged and the supernatant was mixed with organic solvents, *e.g.*, propanol for EGCG and ECG and ethanol for EGC and EC (Fig. S5, ESI†). The final concentration of the organic solvents in the solution was 67% (v/v). The catechin concentration in the solution was measured by a fluorometer. The partition coefficient (PC) was calculated according to eqn (5):

$$PC = \log([C_{mem}]/[C_{sup}]) = \log(([C_{tot}] - [C_{sup}])/[C_{sup}]) \quad (5)$$

$[C_{sup}]$ is the concentration of catechins in the supernatants, and $[C_{tot}]$ the total concentration (10 μM). Thus $[C_{mem}]$, the concentration of catechins interacting with lipid membranes, is given by $[C_{tot}]-[C_{sup}]$ (see details in Fig. S6, ESI†). Taking the bead diameter Φ = 5 μm and the density of porous silica ρ_{silica} = 2.33 g mL^{-1}, the accessible surface area of the silica beads is calculated to be 0.5 m^2 per 1 g of beads. Given the mean area per lipid molecule in a fluid phase (70 Å^2),[47] the amount of lipid molecules on one bead can also be calculated. This allows for the determination of the binding stoichiometry for each catechin derivative.

Flicker spectroscopy

GUVs were incubated with 1 μM catechin derivatives for 3 h at 37 °C and then put into a self-built fluidic chamber at 37 °C. It was confirmed that the change in osmolarity outside of GUVs caused by the addition of catechin solution was negligibly small (<1 mOsm kg^{-1}). Osmolality was measured by a Micro-Digital Osmometer (Type 6 M, Löser, Messtechnik, Berlin, Germany). The microscopy observation was performed with an inverted microscope (Axiovert 200, Carl Zeiss, Göttingen, Germany) equipped with a Plan-Neofluar Antiflex oil-immersion objective (63×, N.A. 1.25). Phase contrast images of GUVs were recorded with an Orca ER CCD camera (Hamamatsu Photonics, Herrsching, Germany) with 60 ms per frame for 30 s. The image analysis was

carried out by using a self-developed routine based on the combination of ImageJ (NIH, Bethesda, MD, USA) and Igor Pro (WaveMetrics, OR, USA). A detailed explanation is provided in the ESI.† First, the position of the GUV edge was determined (Fig. S7, ESI†).[48] Then, the bending stiffness, k_c, of GUVs was determined by Fourier analysis of the fluctuation of the contour of GUV $v(\varphi,t)$ according to the $v(\varphi,t) = R_0 \sum_q v_q(t) e^{-iq\varphi}$ (φ azimuth angle, R_0 mean vesicle radius, q = 0, 1, 2,... wave number).[28–32] The mean square amplitude (MSA) in the equatorial plane as $\langle v_q{}^2 \rangle$ can be expressed as eqn (6):

$$\langle v_q{}^2 \rangle = \frac{k_B T}{k_c} \sum_{l=q}^{l_{max}} \frac{N_{l,q}\left[P_l^q\left(\cos\frac{\pi}{2}\right)\right]^2}{(l+2)(l-1)[l(l+1)+\sigma(\Delta)]} \quad (6)$$

where $\sigma(\Delta)$ is effective tension, and $P_l^q\left(\cos\frac{\pi}{2}\right)$ are the Legendre polynomials in the equatorial plane. $N_{l,q} = \frac{2l+1}{4\pi} \times \frac{(l-q)!}{(l+q)!}$. l_{max} was set to 100. k_c was determined from GUVs showing the bending-dominated regime ($\langle v_q{}^2 \rangle \sim q^{-3}$),[31] which corresponds to $2 \leq q \leq 5$ for EGCG and ECG and $8 \leq q \leq 17$ for control, EGC, and EC (Fig. S8, ESI†). It should be noted that MSA data follow only the q^{-1} power-law (*i.e.*, tension-dominated) were not included in our analysis. Autocorrelation analysis (decay time) was performed for a cross-check of the MSA analysis (Fig. S10, ESI†).

AFM observation of a supported lipid bilayer

A home-built AFM with a commercially available controller (ARC2, Oxford Instruments) was used to observe a supported bilayer of DPPC (1,2-dipalmitoyl-*sn*-glycero-3-phosphocholine) in the absence or presence of EGCG. To prepare a supported lipid bilayer, we first prepared DPPC SUVs (1 mg mL^{-1}) in phosphate buffered saline (PBS, pH = 7.4) by the filter extrusion. Then a mixture of 400 μL of the SUV suspension and 4 μL of 300 mM of a $CaCl_2$ solution was deposited on a freshly cleaved mica substrate with a diameter of 15 mm (V-1 grade, SPI Supplies) that was fixed on an AFM sample cell. The sample cell was incubated at 60 °C for 1–2 h and rinsed with pure PBS after cooling down to a room temperature. AFM measurements were carried out in PBS with or without 5 μM EGCG (final concentration) at room temperature. A Si cantilever (AC240TS, Olympus) with a nominal resonance frequency of 35 kHz and a nominal spring constant of 2 N m^{-1} in liquid was used.

3. Results

3.1 Aggregation of SUVs induced by the catechin derivatives

Fig. 2A shows OPPC SUV suspensions (660 μM) after 24 h incubation with 100 μM EGCG or EC. The incubation with EGCG resulted in the formation of large aggregates (~mm) precipitating on the bottom of the sample tube (left), while the suspension mixed with EC seemed to remain intact (right). This seems to qualitatively agree well with previous studies that

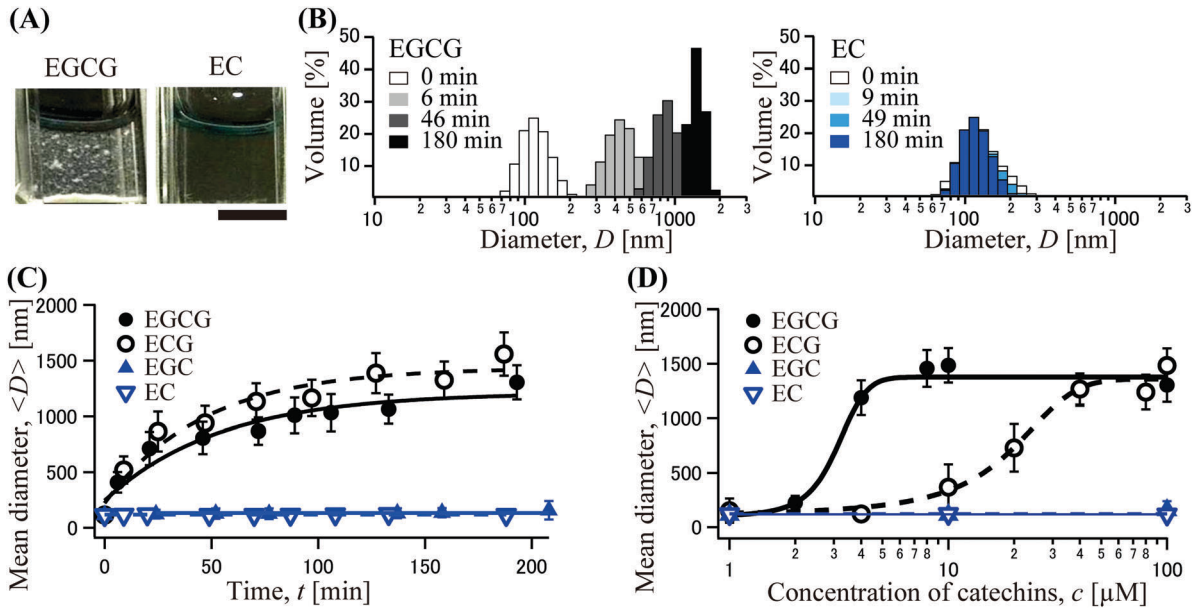

Fig. 2 DLS results of the size of SUV aggregates in the presence of the catechin derivatives. (A) OPPC SUV suspensions (660 μM) after 24 h incubation with 100 μM EGCG and EC. The scale bar is 6 mm. (B) Histogram of the diameters of SUV suspensions (33 μM) with 100 μM EGCG and EC at different incubation time points. (C) Time evolution of the mean diameter of the aggregates (normalized by volume) exposed to 100 μM catechin derivatives. The data points were fitted with the exponential function (eqn (3)) for EGCG/ECG and an equation of a horizontal line for EGC and EC. (D) Mean diameter of aggregates (normalized by volume) exposed to different concentrations of the catechin derivatives (t = 180 min). The data points were fitted with the sigmoidal function (eqn (4)) for EGCG/ECG and an equation of a horizontal line for EGC and EC. Error bars represent standard deviation (σ) calculated according to eqn (2).

reported the increase in the turbidity of vesicle suspensions caused by EGCG.[1,13,14] To quantitatively evaluate the reaction kinetics of membrane aggregation, DLS of a suspension with a lower lipid concentration (~33 μM) was measured over time. Fig. 2B shows the changes in size distribution after mixing with 100 μM EGCG or EC over time. In the case of EGCG, the mean diameter of the aggregates, $\langle D \rangle$, exhibited a clear increase within the first 6 min ($\langle D \rangle \sim 400$ nm), which further shifted to $\langle D \rangle \sim 1$ μm ($t \sim 180$ min). On the other hand, neither the mean diameter ($\langle D \rangle \sim 100$ nm) nor the standard deviation ($\sigma \sim 30$ nm) of the size distribution showed any change in the presence of EC. Fig. 2C shows the time evolution of the mean diameter $\langle D \rangle$ of aggregates (normalized by volume), exposed to the different catechin derivatives (100 μM). As presented in Fig. 2C, the mixing with EGC (solid blue symbols) and EC (open blue symbols) solutions did not lead to any detectable shift in $\langle D \rangle$ over 180 min. However, with the mixing of EGCG (solid black symbols), $\langle D \rangle$ shows an exponential increase with a characteristic time constant of $\tau \sim 68$ min according to eqn (3). $\langle D \rangle$ also increased in the presence of ECG (open black symbols) within a comparable timescale ($\tau \sim 54$ min). In parallel, we determined the critical concentration level of each catechin necessary to induce membrane aggregation. In Fig. 2D, we plotted the mean diameter $\langle D \rangle$ of aggregates at $t = 180$ min as a function of catechin concentrations (1–100 μM), and the experimental data points were fitted with eqn (4). First, the catechin derivatives without the galloyl moiety (EC and EGC, blue triangles) exhibited no clear sign of interactions at concentrations of 1–100 μM catechin, as indicated in Fig. 2D. In contrast, the critical EGCG concentration causing vesicle aggregation, $c_{\text{half-EGCG}} = 3$ μM, was distinctly smaller than that of ECG ($c_{\text{half-ECG}} = 19$ μM). The more significant EGCG interactions compared to ECG might be attributed to an additional influence by the hydroxyl groups in the B ring.

3.2 Influence of the catechin derivatives on surface tension and phase behavior

Fig. 3A shows the changes in the surface pressure of OPPC monolayers caused by the injection of 100 μM EGCG (black) or EC (blue), monitored at a constant film area and thus at a constant area per molecule ($A = 63$ Å^2). Prior to the experiments, we confirmed that the catechin derivatives alone (Fig. S2, ESI†)[43] and TFE (Fig. S3, ESI†) have no surface activity. The injection of EGCG into the subphase at $t = 15$ min led to a slow increase in the surface pressure, reaching a saturation level at $t \sim 200$ min. However, despite the fact that the time needed for the saturation in Fig. 2C and 3A seems similar, the comparison of the reaction kinetics in these two cases is invalid in terms of dimensionality. In Fig. 2C, we recorded the binding of soluble catechin molecules to vesicles suspended in 3D (bulk), while the results presented in Fig. 3A reflect the adsorption of catechin molecules to a 2D monolayer surface.[49,50] Fig. 3B shows the increase in surface pressure ($\Delta\pi$) from $t = 0$ min to $t = 200$ min, plotted as a function of the concentration of catechin derivatives. EGCG and EGC resulted in distinct increases in the surface pressure (7–10 mN m^{-1}) at $c = 100$ μM, suggesting that the

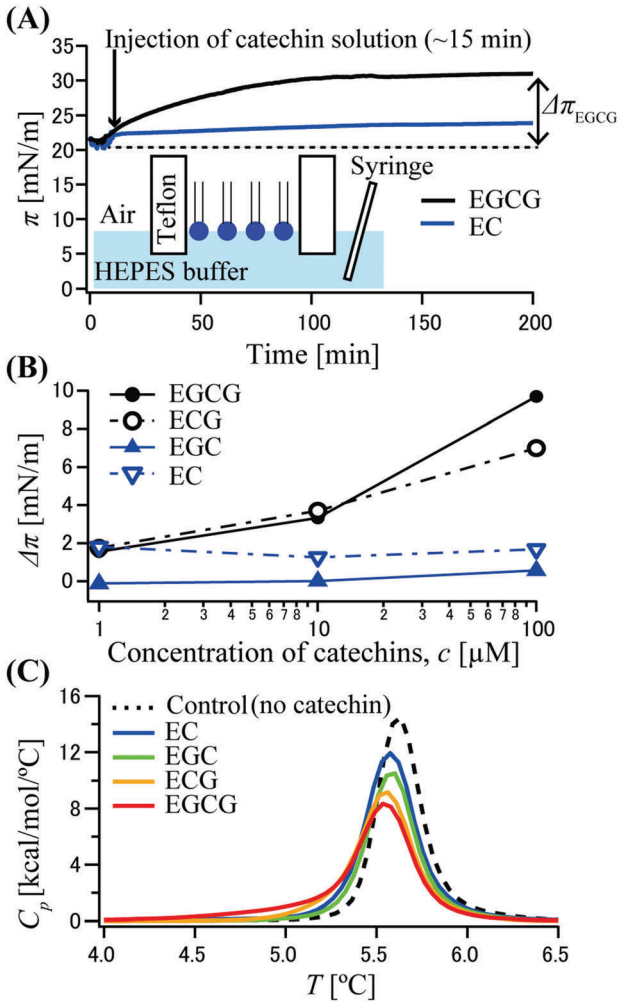

Fig. 3 (A) Time evolution of the surface pressure of OPPC monolayers. EGCG or EC solutions were injected into the subphase after the stabilization of monolayer ($t \sim 15$ min). The final concentration of EGCG and EC was 100 μM. A schematic illustration of the experimental system is displayed in the graph. (B) Increase in surface pressure ($\Delta\pi$) at $t = 200$ min with different concentrations of catechin derivatives. (C) Heat capacity (C_p) scans of 2 mM SOPC SUV suspensions with 10 μM catechin derivatives.

catechins with the galloyl moiety do not only adsorb on the membrane surface but also intercalate into the membrane core at such a high concentration. This behavior is similar to the intrusion of antimicrobial peptides into lipopolysaccharide monolayers.[51–53] The fact that the monolayer seemed to remain intact in the presence of EC and EGC seems consistent with the DLS results presented in Fig. 2. Our findings presented in Fig. 2 and 3 suggest that only the catechin derivatives with the galloyl moiety (EGCG and ECG) strongly interact with lipid membranes. This leads us to the next question: how deeply do catechin derivatives get into the membrane core? To address this issue, we determined the thermotropic phase behavior of SOPC vesicles in the absence and presence of the catechin derivatives by using DSC. Fig. 3C shows heat capacity (C_p) scans of 2 mM SOPC SUV suspensions with 10 μM catechin derivatives. All types of catechin derivatives slightly decreased the main phase transition temperature (T_m) and broadened the peak width.

Such a tendency seems to be more pronounced for EGCG and ECG compared to EC and EGC, which is consistent with previous DSC studies using lipids with saturated alkyl chains.[26,54] Nevertheless, the fact that the main phase transition is not completely damped suggests that, in a low concentration regime ($\leq$10 μM), the catechin molecules do not significantly cause the disordering of hydrocarbon chains in the membrane core like other substitutional impurities such as cholesterols and anesthetics.[55]

3.3 Affinity of the catechin derivatives to lipid membranes

In the next step, the affinity of the four catechin derivatives to lipid membranes were systematically compared using silica particles coated with various lipid membranes.[44] As schematically presented in Fig. 4A, the catechin molecules bound to the particle-supported membrane can be easily separated from the unbound molecules in supernatants owing to a clear difference in the density between silica and aqueous buffer.[44–46] As a measure of affinity, the partition coefficient (PC) was calculated according to eqn (3). As shown in Fig. 4B, the order of the PCs for the different catechins was ECG > EGCG > EGC > EC. First, a clear difference between the catechin derivatives with (EGCG, EGC) and without the galloyl moiety (EC, EGC) indicates that the galloyl moiety plays a key role in the binding of the catechin derivatives to the lipid membrane. On the other hand, a slight difference in the affinity between ECG and EGCG suggests that the hydroxyl groups on the B ring do not have a major impact on catechin–membrane interactions.

Do the galloyl catechin derivatives (EGCG and ECG) specifically interact with the phosphatidyl choline moiety? Or is there any lipid that shows a stronger affinity? To answer this question, we investigated the influence of the net electric charges of lipid head groups. There have been several reports on the interaction of catechins with SUVs of egg-PC containing anionic phosphatidyl serine from the bovine brain or a cationic surfactant (stearylamine),[1,21] but the use of lipid mixtures with different chain lengths and head groups makes it difficult to elucidate membrane–catechin interactions. Here, we prepared DOPC vesicles incorporating 30 mol% of lipids possessing the same dioleoyl chains (C18:1 *cis*) but different head groups: DOTAP (+), DOPE (±), and DOPG (−). The membranes were deposited on silica particles and the partition coefficients and the binding stoichiometry of EGCG were determined following the procedure shown in Fig. 4A. As shown in Fig. 4D, we found that the membranes doped with DOTAP (+) have a comparable affinity to those with pure DOPC (control, (±)). Interestingly, the membranes incorporating zwitterionic DOPE (±) exhibited a distinctly lower EGCG affinity than those with DOPC. This finding cannot be explained simply in terms of electrostatic interactions, because both DOPC and DOPE are zwitterionic. One possible reason could be the difference in the packing of lipid molecules between bulkier choline groups and more compact ethanolamine groups,[56] resulting in different spatial accessibility of EGCG molecules. On the other hand, the membranes doped with DOPG (−) exhibited the lowest EGCG affinity compared to the other three systems, suggesting that neutral glycerol connected to the phosphate (−) is less attractive to EGCG.

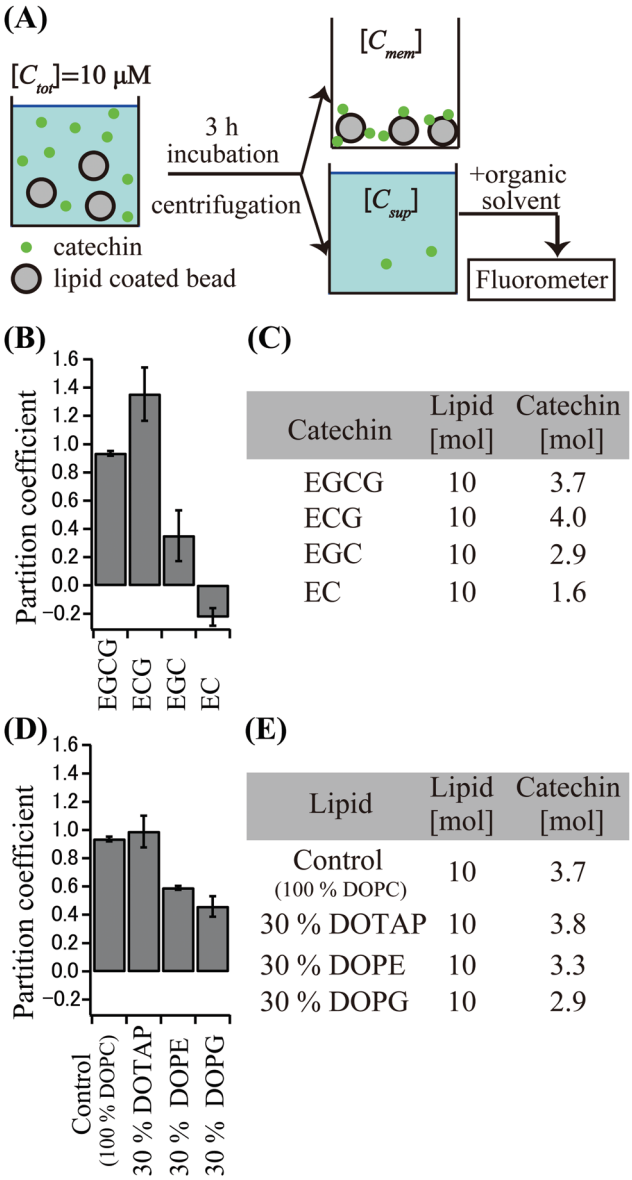

Catechin	Lipid [mol]	Catechin [mol]
EGCG	10	3.7
ECG	10	4.0
EGC	10	2.9
EC	10	1.6

Lipid	Lipid [mol]	Catechin [mol]
Control (100 % DOPC)	10	3.7
30 % DOTAP	10	3.8
30 % DOPE	10	3.3
30 % DOPG	10	2.9

Fig. 4 (A) Schematic illustration of the experimental procedure for the evaluation of partition coefficients. The concentration of DOPC lipids was calculated to be 24 μM. (B) Partition coefficients of 10 μM catechin derivatives (n = 3) and (C) the corresponding stoichiometry. (D) Partition coefficients of 10 μM EGCG to lipids with different head groups and (E) the corresponding stoichiometry. The error bar represents standard deviation.

This seems to agree well with a previous NMR study, suggesting that the galloyl moiety interacts with the quaternary amine of the PC head group *via* cation–π interactions.[15]

3.4 Impact of the catechin derivatives on membrane mechanics

In the final step, we studied how the catechin derivatives affect the mechanical properties of lipid membranes. Using flicker spectroscopy (Fig. S7, S8 and ESI,† Movies),[28–32] we determined the bending stiffness (k_c) of GUVs in the presence of catechin derivatives. Fig. 5A shows histograms of k_c of GUV in the absence and presence of 1 μM catechin derivatives. The histogram

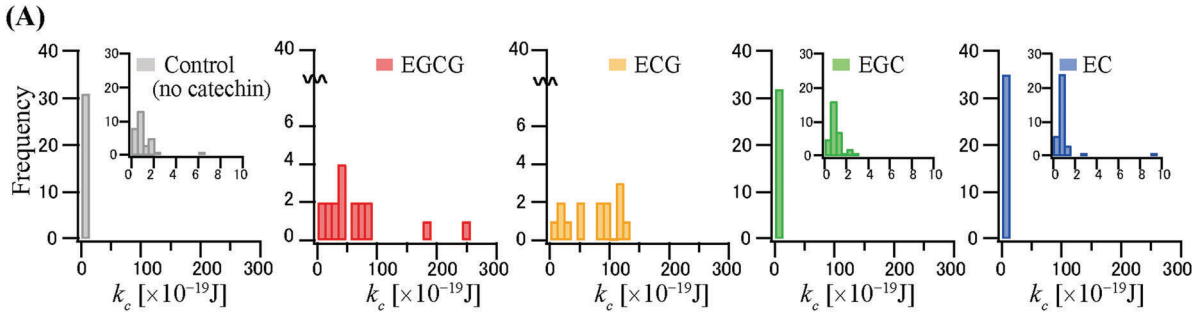

Catechin derivatives	Control (no catechin)	EGCG	ECG	EGC	EC
k_c [×10^{-19}J]	1.1 ± 1.1	61.2 ± 60.7	69.9 ± 42.4	0.9 ± 0.6	1.0 ± 1.5

Fig. 5 Evaluation of the mechanics of GUVs with catechin derivatives. (A) Histograms of the bending stiffness (k_c) of OPPC GUVs without/with 1 μM catechin derivatives. The insets show magnification of the histograms. (B) Summary of the mean k_c ± standard deviation of GUVs without/with 1 μM catechin derivatives.

of k_c for intact GUVs (control) shows a maximum at $k_c \sim 0.8 \times 10^{-19}$ J, which is in good agreement with the previously reported k_c of fluid membranes.[32] In the cases of EC (blue) and EGC (green) without the galloyl moiety, the histograms show the maximum values that are comparable to that of intact GUVs, $k_c \sim 0.8 \times 10^{-19}$ J. On the other hand, we found that the exposure of GUVs to EGCG (red) and ECG (orange) with galloyl moieties resulted in a significant stiffening of membranes: in both cases the mean values of k_c are more than 60 times higher than those of the other samples (Fig. 5B). Such stiffening of lipid membranes with EGCG and ECG could also be detected by autocorrelation analysis (Fig. S10, ESI†). It should be noted that the increase in osmolality caused by the injection of catechin solutions (<1 mOsm kg^{-1}) was negligibly small. Also, no aggregation or lysis of GUVs was found, as the EGCG concentration used in this study (1 μM) is 30 times lower than that in a previous study.[13] Moreover, the significant increase (not decrease) in bending stiffness with no detectable areal expansion (<4%) also excluded the possibility of membrane thinning or partial loss of lipids as suggested previously.[14]

4. Discussion

Our results clearly indicate that the catechin derivatives functionalized with a galloyl moiety (EGCG and ECG) show stronger interactions with lipid membranes compared to EC and EGC without a galloyl moiety (Fig. 2–4). The catechin–membrane interaction is dominated by the electrostatic and cation–π interactions between galloyl catechins and quaternary amine groups (Fig. 4). Moreover, the stiffening of membranes caused by EGCG and ECG presented in Fig. 5 suggests the physical role of catechin derivatives in their cancer preventive activity. Recent biophysical studies have revealed that metastatic cancer cells are softer than normal cells of same tissues.[24,57] It is considered that such softness of cancer cells is involved in the mechanism of cancer metastasis where soft and thus deformable cancer cells should be advantageous for the invasion in tissues. Along this line, recent AFM indentation experiments by Suganuma *et al.* demonstrated that the incubation with EGCG leads to an increase in the Young's modulus of melanoma and lung cancer cells, resulting in reduced motility.[23,58,59] Although the cytoskeleton is one of the key components that determine cell mechanics,[24,60] our finding potentially suggests that the significant stiffening of cell membranes also plays a critical role in the suppression of metastasis of cancer cells even in the absence of biochemical cues. Such biophysical effects are in contrast to the known cancer preventive activity of EGCG *via* biochemical pathways.[12,19,20]

The significant increase in the bending stiffness of the membranes suggested the adsorption of aggregates onto the membrane surface, rather than monomers. In fact, AFM revealed that lipid membrane surfaces were covered with fibril- or pancake-like EGCG aggregates with a height of less than ~10 nm (Fig. 6). Such catechin aggregates on lipid membranes should have originated from the ones that were formed in aqueous buffer, which is suggested by our fluorescence spectral data (Fig. S5A, ESI†) and a previous study with galloyl catechin derivatives (EGCG and ECG).[61] Although the presence of lipid vesicles was found to partially dissociate EGCG/ECG aggregates (Fig. S11, ESI†), CD spectra of the galloyl catechin derivatives showed a strong negative Cotton effect around 270–280 nm, corresponding to π–π* transition (Fig. 7A and B). In contrast, no sign of aggregates on membranes was found for EGC and EC without a galloyl moiety (Fig. 7C and D). Therefore, the significant membrane stiffening caused by galloyl catechins can be interpreted in terms of the adsorption of catechin aggregates, resulting in an increase in the apparent mass of the membranes and/or by the formation of two dimensional networks on the membranes (Fig. 8). In fact, the stiffening of lipid membranes by two dimensional molecular aggregates on the membrane surface was also found in other systems, such as the stiffening of vesicles coated with streptavidin crystals.[62]

Cholesterol, a vital component of biological membranes, has also been well-known to increase the bending stiffness of fluid lipid membranes by intercalating between hydrocarbon chains.[63,64]

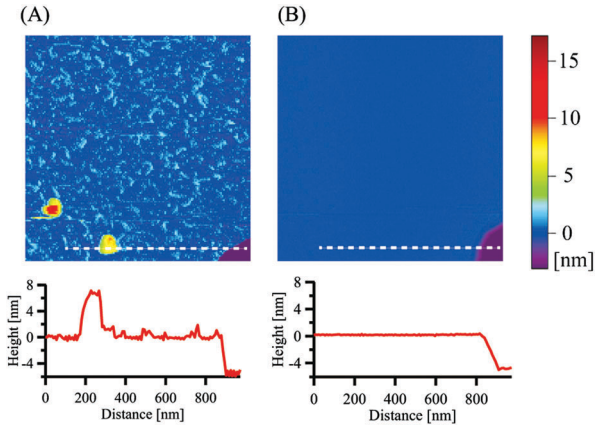

Fig. 6 AFM images (1.2 μm × 1.2 μm) of the DPPC bilayer in the (A) presence and (B) absence of 5 μM EGCG. The corresponding height profiles along the dotted while lines in the AFM images are provided at the bottom.

When the molar fraction exceeds 30%, lipid molecules take a so-called liquid ordered phase.[47] Previous studies with DSC and fluorescence spectroscopy also suggested that the vesicles made using a dry mixture of an extremely high concentration of ECG (≥15 mol%) and lipids may induce the formation of well-packed lipid domains.[26] However, our DSC results showed that the addition of catechin at physiologically relevant concentration (~0.5 mol%, Fig. 3) to vesicle suspensions led to only a slight decrease in T_m, accompanied by a broadening of the main transition peak in the presence of all catechin derivatives. Although this tendency was slightly more pronounced in the presence of EGCG and ECG, our data indicate that the catechin derivatives do not significantly cause the disordering of hydrocarbon chains. Therefore, we concluded that the membrane stiffening was not dominated by the incorporation of catechins into the hydrocarbon chains.

Mertins *et al.* reported that chitosan, a cationic polysaccharide, binds to negatively charged and neutral phospholipids and reduces the fluctuation of DOPC GUVs,[65] which was theoretically predicted for charged lipid membranes.[66] However, this scenario also does not seem realistic in our catechin system, because the binding stoichiometry of EGCG and DOTAP (+) membranes, [EGCG]:[DOTAP] = 3.8:10, was the same as that with DOPC (±), [EGCG]:[DOPC] = 3.7:10 (Fig. 4E). Moreover, the increase in bending stiffness caused by EGCG ($k_c = 61.2 \times 10^{-19}$ J) and ECG ($k_c > 69.9 \times 10^{-19}$ J) was much larger than that caused by chitosan ($k_c = 3.5 \times 10^{-19}$ J), despite the fact that the degree of protonation of chitosan ($pK_a = 6$–6.5)[67] in the acidic sucrose solution (pH = 4.7) was much higher than that of EGCG ($pK_{a1} = 7.68$) and ECG ($pK_{a1} = 7.76$)[68] in our experimental system (pH ~ 7). Thus we concluded that the adsorption of aggregates onto the membrane surface (Fig. 8, right) plays a dominant role in the increase of the bending stiffness of membranes. Further fine structure studies, such as freeze fracture electron microscopy, could potentially unravel more

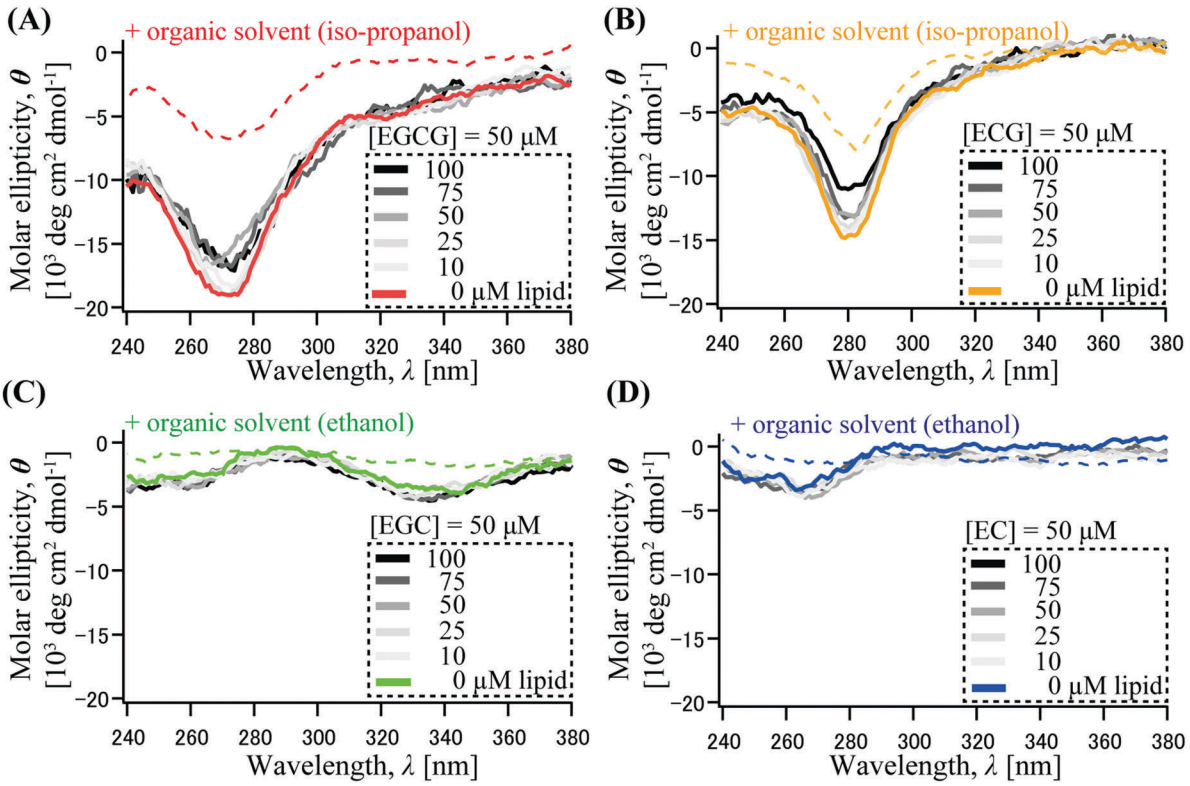

Fig. 7 CD spectra of the catechin derivatives (50 μM in final) with the different concentrations of DOPC SUVs in HEPES buffer solutions. Dotted lines in each graph show CD spectra of the catechin derivatives in the HEPES solution with organic solvents (77% v/v in final).

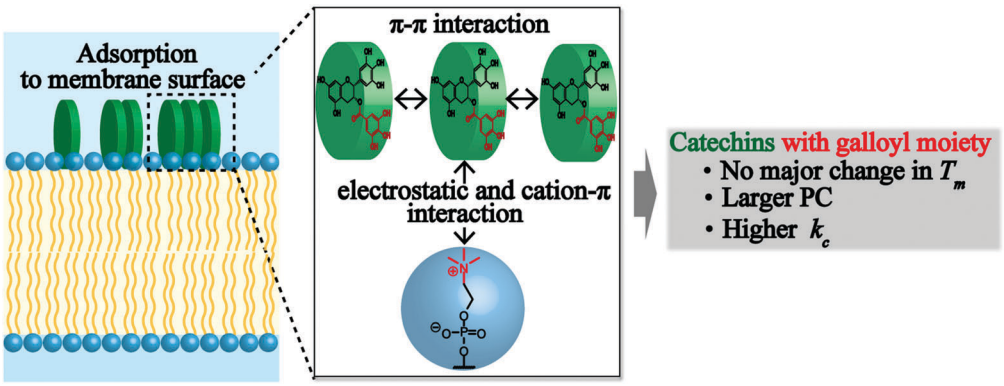

Fig. 8 Models of molecular interactions between catechin derivatives with the galloyl moiety and phospholipid membranes. Galloyl catechins are not significantly incorporated into the hydrocarbon chain region but form aggregates in aqueous solutions and their absorption onto the membrane surface seems to cause significant stiffening of lipid membranes. In contrast, catechins without the galloyl moiety do not form aggregates or stiffen the membrane, suggesting a strong correlation between aggregate formation and membrane stiffening.

detailed insights into how the balance between catechin–lipid and catechin–catechin interactions determines membrane mechanics.

5. Conclusions

In this work, we quantitatively evaluated the physical interactions of catechin derivatives with cell membrane models. By varying the chemical structures of lipids and catechins systematically, we could determine the dominant molecular factors that govern catechin–membrane interactions. Shedding light on the chemical structures of catechin derivatives, we found that the galloyl moiety is the essential structural motif for interactions with phosphatidyl choline membranes, while the additional hydroxyl groups in the B ring do not have a remarkable impact. On the other hand, the fact that the partition coefficients of EGCG were similar between DOTAP (+) and DOPC (±) suggested that electrostatic interactions are not sufficient to account for catechin–membrane interactions, suggesting the contribution of cation–π interactions between galloyl catechins and quaternary amine groups.

In contrast to commonly taken biochemical interpretations to the therapeutic function of catechin molecules such as antioxidant activity and specific inhibition of tumor-related proteins, our flicker spectroscopy provided the first quantitative evidence that the interaction of the galloyl catechins (EGCG and ECG) and membranes leads to a significant increase in the bending stiffness of the lipid membranes by a factor of more than 60, while the catechins without the galloyl moiety have almost no effect. AFM and CD spectroscopy suggest the adsorption of EGCG/ECG aggregates onto the membrane surface. On the other hand, the catechins without the galloyl moiety (EC and EGC) do not form aggregates or cause membrane stiffening, suggesting that the aggregate formation is correlated with the membrane stiffening. As DSC results suggested that the catechin derivatives do not cause the complete disordering of hydrocarbon chains, we concluded that the absorption of galloyl catechin aggregates on the membrane surface plays a dominant role in the significant stiffening of lipid membranes. It should be noted that the catechin concentration studied for membrane mechanics ($\sim$1 μM) is much lower than those used in previous studies, comparable to the level in human blood plasma after green tea consumption (0.1–0.6 μM).[69–71] Therefore, our experimental data demonstrate that the physical interactions with cell membranes should be taken into account in understanding of the pharmaceutical functions of catechin derivatives, such as the prevention of cancer metastasis. In fact, recent studies reported several drugs whose functions are also related to the physical interaction with cell membranes.[48,72–75] For example, antiseptic peptide P19 moderates the changes in the spring constant and bending stiffness of red blood cell membranes with endotoxin.[48] Tamoxifen, an important anticancer drug for breast cancer, increases the area compressibility modulus of lipid bilayers.[75] Our study together with these reports clearly suggests the importance of drug designs on the basis of not only biochemical effects but also physicochemical effects.

Acknowledgements

The present work was supported by grants from the Japan Society for the Promotion of Science (JSPS) KAKENHI (No. 15H05351, 16K12868, 23106005, and 26103521). M. T. thanks the Phospholipid Research Center for the support. A. M. is thankful to the Alexander von Humboldt Foundation for the support. M. T. is an investigator of the German Excellence Cluster "CellNetwork". The iCeMS is supported by the World Premier International Research Center Initiative (WPI), MEXT, Japan. T. M. and H. I. thank JSPS for Grants-in-Aid (No. 25 8820 and 25 1297). H. Y. Y., N. K., and M. S. are thankful for the grant from the Takeda Science Foundation.

References

1 H. Ikigai, T. Nakae, Y. Hara and T. Shimamura, *Biochim. Biophys. Acta*, 1993, **1147**, 132.
2 C. N. Gordon and W. D. Wareham, *Int. J. Antimicrob. Agents*, 2010, **36**, 129.

3 L. Zhao, W. Li, S. Zhu, S. Tsai, J. Li, J. K. Tracey, P. Wang, S. Fan, E. A. Sama and H. Wang, *Inflammation Allergy: Drug Targets*, 2013, **12**, 308.
4 S. Bettuzzi, M. Brausi, F. Rizzi, G. Castagnetti, G. Peracchia and A. Corti, *Cancer Res.*, 2006, **66**, 1234.
5 M. Shimizu, Y. Fukutomi, M. Ninomiya, K. Nagura, T. Kato, H. Araki, M. Suganuma, H. Fujiki and H. Moriwaki, *Cancer Epidemiol., Biomarkers Prev.*, 2008, **17**, 3020.
6 A. S. Tsao, D. Liu, J. Martin, M. X. Tang, J. J. Lee, K. A. Ei-Naggar, I. Wistuba, S. K. Culotta, L. Mao and A. Gillenwater, *et al.*, *Cancer Prev. Res.*, 2009, **2**, 931.
7 A. Sugisawa and K. Umegaki, *J. Nutr.*, 2002, **132**, 1836.
8 Y. Saffari and H. M. S. Sadrzadeh, *Life Sci.*, 2004, **74**, 1513.
9 Z. Hou, S. Sang, H. You, J. M. Lee, J. Hong, V. K. Chin and S. C. Yang, *Cancer Res.*, 2005, **65**, 8049.
10 J. Jankun, H. S. Selman and R. Swiercz, *Nature*, 1997, **387**, 561.
11 S. Garbisa, S. Biggin, N. Cavallarin, L. Sartor, R. Benelli and A. Albini, *Nat. Med.*, 1999, **5**, 1216.
12 S. C. Yang, X. Wang, L. Gang and C. S. Picinich, *Nat. Rev. Cancer*, 2009, **9**, 429.
13 Y. Tamba, S. Ohba, M. Kubota, H. Yoshioka, H. Yoshioka and M. Yamzaki, *Biophys. J.*, 2007, **92**, 3178.
14 Y. Sun, C. W. Hung, Y. F. Chen, C. C. Lee and W. H. Huang, *Biophys. J.*, 2009, **96**, 1026.
15 Y. Uekusa, K. M. Ishijima, O. Sugimoto, T. Ishii, S. Kumazawa, K. Nakamura, K. Taniji, A. Naito and T. Nakayama, *Biochim. Biophys. Acta*, 2011, **1808**, 1654.
16 S. Okabe, M. Suganuma, M. Hayahsi, E. Sueoka, A. Komori and H. Fujiki, *Jpn. J. Cancer Res.*, 1997, **88**, 639.
17 K. Mabe, M. Yamada, I. Oguni and T. Takahashi, *Antimicrob. Agents Chemother.*, 1999, **43**, 1788.
18 S. Lamy, D. Gingras and R. Béliveau, *Caner Res.*, 2002, **62**, 381.
19 H. Tachibana, K. Koga, Y. Fujimura and K. Yamada, *Nature*, 2004, **11**, 380.
20 H. Fujiki, *Chem. Rec.*, 2005, **5**, 119.
21 K. Kajiya, S. Kumazawa and T. Nakayama, *Biosci., Biotechnol., Biochem.*, 2002, **66**, 2330.
22 M. Kamihira, H. Nakazawa, A. Kira, Y. Mizutani, M. Nakamura and T. Nakayama, *Biosci., Biotechnol., Biochem.*, 2008, **72**, 1372.
23 T. Watanabe, H. Kuramochi, A. Takahashi, K. Imai, N. Katsuta, T. Nakayama, H. Fujiki and M. Suganuma, *J. Cancer Res. Clin. Oncol.*, 2012, **138**, 859.
24 E. S. Cross, S. Y. Jin, Y. Q. Lu Y. J. Rao and K. J. Gimzewski, *Nanotechnology*, 2011, **22**, 215101.
25 H. Tsuchiya, *Pharmacology*, 1999, **59**, 34.
26 N. Caturla, V. E. Samper, J. Villalaín, R. C. Mateo and V. Micol, *Free Radical Biol. Med.*, 2003, **34**, 648.
27 L. Palacios, H. Rosado, V. Micol, E. A. Rosato, P. Bernal, R. Arroyo, H. Grounds, C. J. Anderson, A. R. Stabler and W. P. Taylor, *PLoS One*, 2014, **9**, e93830.
28 F. Brochard and J. F. Lennon, *J. Phys.*, 1975, **36**, 1035.
29 P. H. Duwe and E. Sackmann, *Physica A*, 1990, **16**, 410.
30 H. Strey, M. Peterson and E. Sackmann, *Biophys. J.*, 1995, **69**, 478.
31 W. Häckl, U. Seifert and E. Sackmann, *J. Physiol.*, 1997, **7**, 1141.
32 U. Seifert, Configurations of fluid membranes and vesicles, *Adv. Phys.*, 1997, **46**, 13.
33 S. W. F. Stetter and T. Hugel, *Biophys. J.*, 2013, **104**, 1049.
34 S. R. Gracià, N. Bezlyepkina, L. R. Knorr, R. Lipowsky and R. Dimova, *Soft Matter*, 2010, **6**, 1472.
35 J. D. Stark, C. T. Killian and M. R. Raphael, *Phys. Biol.*, 2011, **8**, 056008.
36 E. M. Solmaz, S. Sankhagowit, R. Biswas, A. C. Mejia, L. M. Povinelli and N. Malmstadt, *RSC Adv.*, 2013, **3**, 16632.
37 D. A. Bangham, M. M. Standish and C. J. Watkins, *J. Mol. Biol.*, 1965, **13**, 238.
38 J. M. Hope, B. M. Bally, G. Webb and R. P. Cullis, *Biochim. Biophys. Acta*, 1985, **812**, 55.
39 L. Saunders, J. Perrin and B. D. Gammack, *J. Pharm. Pharmacol.*, 1962, **14**, 567.
40 B. M. Abramson, R. Katzman and P. H Gregor, *J. Biol. Chem.*, 1964, **239**, 70.
41 I. M. Angelova, S. Soleau, P. Meleard, F. J. Faucon and P. Bothorel, *Prog. Colloid Polym. Sci.*, 1992, **89**, 127.
42 L. Mathivet, S. Cribier and F. P. Devaux, *Biophys. J.*, 1996, **70**, 1112.
43 P. Sausse, A. V. Béghin and R. Douillard, *Langmuir*, 2003, **19**, 737.
44 A. Loidl-Stahlhofen, S. Kaufmann, T. Braunschweig and M. T. Bayeri, *Nature*, 1996, **14**, 999.
45 S. Kaufmann, M. I. Weiss and M. Tanaka, *J. Am. Chem. Soc.*, 2007, **129**, 10807.
46 M. Tutus, S. Kaufmann, M. I. Weiss and M. Tanaka, *Adv. Funct. Mater.*, 2012, **22**, 4873.
47 R. Lipowsky and E. Sackmann, *Structure and Dynamics of Membranes*, Elsevier, Amsterdam, 1995.
48 H. Ito, N. Kuss, E. B. Rapp, M. Ichikawa, T. Gutsmann, K. Brandenburg, B. M. J. Pöschl and M. Tanaka, *J. Phys. Chem. B*, 2015, **119**, 7837.
49 L. S. Harddt, *Biophys. Chem.*, 1979, **10**, 239.
50 M. Tanaka, *Curr. Opin. Colloid Interface Sci.*, 2013, **18**, 432.
51 G. R. Oliveira, E. Schneck, E. B. Quinn, V. O. Konovalov, K. Brandenburg, U. Seydel, T. Gill, B. C. Hanna, A. D. Pink and M. Tanaka, *C. R. Chim.*, 2009, **12**, 209.
52 G. R. Oliveira, E. Schneck, E. B. Quinn, V. O. Konovalov, K. Brandenburg, T. Gutsmann, T. Gill, A. D. Pink and M. Tanaka, *Phys. Rev. E: Stat., Nonlinear, Soft Matter Phys.*, 2010, **81**, 041901.
53 W. Abuillan, E. Schneck, A. Körner K. Brandenburg, T. Gutsmann, T. Gill, A. Vorobiev, O. Konovalov and M. Tanaka, *Phys. Rev. E: Stat., Nonlinear, Soft Matter Phys.*, 2013, **88**, 012705.
54 V. Abram, B. Berlec, A. Ota, M. Sentjurc, P. Blatnik and P. N. Ulrich, *Food Chem.*, 2013, **139**, 804.
55 M. Tanaka, A. Jutila and J. K. P. Kinnunen, *J. Phys. Chem. B*, 1998, **102**, 5358.
56 J. N. Israelachvili, *J. Chem. Soc., Faraday Trans.*, 1976, **2**, 72–1525.
57 E. S. Cross, S. Y. Jin, J. Rao and K. J. Gimzewski, *Nat. Nanotechnol.*, 2007, **2**, 780–783.

58 A. Takahashi, T. Watanabe, A. Mondal, K. Suzuki, M. Kanno, Z. Li, T. Yamazaki, H. Fujiki and M. Suganuma, *Biochem. Biophys. Res. Commun.*, 2014, **443**, 1.
59 M. Suganuma, A. Takahashi, T. Watanabe, K. Iida, T. Matsuzaki, H. Y. Yoshikawa and H. Fujiki, *Molecules*, 2016, **21**, 1566.
60 J. Guck, S. Schinkinger, B. Lincoln, F. Wottawah, S. Ebert, M. Romeylke, D. Lenz, H. Erickson, R. Anathakrishnan and D. Mitchell, *et al.*, *Biophys. J.*, 2005, **88**, 3689.
61 K. Kitano, Y. K. Nam, S. Kimura, H. Fujiki and Y. Imanishi, *Biophys. Chem.*, 1997, **65**, 157.
62 P. Ratanabanangkoon, M. Gropper, R. Merkel, E. Sackmann and P. A. Gast, *Langmuir*, 2003, **19**, 1054.
63 E. Evans and W. Rawicz, *Phys. Rev. Lett.*, 1990, **64**, 2094.
64 J. Henriksen, C. A. Rowat and H. J. Iosen, *Eur. Biophys. J.*, 2004, **33**, 732.
65 O. Mertins and R. Dimova, *Langmuir*, 2013, **29**, 14552.
66 M. Winterhalter and W. Helfrich, *J. Phys. Chem.*, 1992, **96**, 327.
67 S. K. C. Pillai, W. Paul and P. C. Sharma, *Prog. Polym. Sci.*, 2009, **34**, 641.
68 M. Muzolf, H. Szymusiak, G. A. Swinglo, M. C. M. I. Rioetjens and B. Tyrakowska, *J. Agric. Food Chem.*, 2008, **56**, 816.
69 S. C. Yang, *Nature*, 1997, **389**, 134.
70 S. C. Yang, L. Chen, J. M. Lee, D. Balentine, C. M. Kuo and P. S. Schantz, *Cancer Epidemiol., Biomarkers Prev.*, 1998, **7**, 351.
71 Y. Cao and R. Cao, *Nature*, 1999, **398**, 381.
72 N. Frenkel, A. Makky, I. R. Sudji, M. Wink and M. Tanaka, *J. Phys. Chem. B*, 2014, **118**, 14632–14639.
73 M. Kucio, J. L. F. C. Lima and S. Reis, *Curr. Med. Chem.*, 2010, **17**, 1795–1809.
74 K. U. Maheswari, T. Ramachandran and D. Rajaji, *Biochim. Biophys. Acta*, 2000, **1463**, 230–240.
75 N. K. Khadka, X. Cheng, C. S. Ho, J. Katsaras and J. Pan, *Biophys. J.*, 2015, **108**, 2492–2501.